Kovove Mater. 54 2016 107–112
DOI: 10.4149/km_2016_2_107

Synthesis and characterization of CeO_2-doped ZnO

H. Colak

Cankiri Karatekin University, Faculty of Science, Department of Chemistry, Cankiri 18100, Turkey

Received 8 August 2014, received in revised form 28 February 2015, accepted 2 April 2015

Abstract

This paper reports the synthesis, crystal structure and electrical properties of CeO_2-doped ZnO powders. X-ray diffraction shows that majority of the samples are *monophase* and have the cubic structure. The solubility limit of Ce^{4+} ions in ZnO lattice was found to be 3 mol% (after heating at 1000 °C), whereby the impurity phase was determined to be the cubic-CeO_2. For *monophase* CeO_2-doped ZnO samples synthesized at 1000 °C, the lattice parameters a and c increased with increasing CeO_2 concentration. The electrical conductivity of undoped ZnO and all *monophase* samples was measured using the four-probe method. The electrical conductivity was increased with both temperature and CeO_2 doping. Also, the activation energy of all the *monophase* samples was calculated. Type of the activation energy of all the *monophase* samples is thermal. The values were found to be in the range from 0.458 to 0.302 eV for the low-temperature region and from 0.989 to 1.132 eV for the high-temperature region.

K e y w o r d s: zinc oxide, doping zinc oxide, electrical conductivity, solid state method

1. Introduction

Zinc oxide (ZnO) is commonly used in photovoltaic devices as a transparent conductive oxide (TCO) owing to its electrical and optical properties. Also, ZnO is a non-toxic material and has low-cost synthesis [1]. For applications and control over the electrical and optical properties, doping with different metals is needed [2]. In this way, the effect of doping can enhance the properties of ZnO and enable the design of new applications [1]. Besides, heating treatment is a commonly used method to enhance crystal quality and to study structural defects in materials. For semiconductors, heating treatment is also used to activate doping materials. During the heating process, dislocations and other structural defects move in the material, and adsorption/decomposition occurs on the surface. Thus the structure and the stoichiometric ratio of the material change, which affects the electrical and optical characteristics of ZnO [3].

To improve the electrical and optical properties of the ZnO, multivalent metal ions have been used as the doping metals [1]. Rare earth metals are suitable for tailoring the electrical and optical properties because they have higher oxidation state and lower ionic radius than Zn^{2+}. Also, doping causes an increase in the conductivity of the ZnO. Doping of ZnO is achieved by replacing Zn^{2+} ions with ions of dopant metals [2]. Ce^{4+} ions have unique optical characteristics, and this property makes them an ideal dopant.

In this study, the effect of the doping amount of CeO_2 on structural and electrical properties of ZnO is investigated. The samples were synthesized by the solid state method at high temperatures and characterized for their structural, morphological and electrical properties. To investigate the solubility of CeO_2 in ZnO lattice, ten different compositions of solid oxide mixtures were annealed at varying temperatures. Solid state reaction was chosen because of its reproducibility, easy control and the ability to yield sufficient products for characterization measurements [4].

2. Experimental study

At first, solid oxide mixtures of CeO_2-ZnO (in the range of 1–10 mol%) were prepared by mixing and homogenizing, with a stoichiometric ratio of pure ZnO

*Corresponding author: tel.: +90 376 218 95 37/Ext: 8050; fax: +90 376 218 95 41;
e-mail address: hakancolak@karatekin.edu.tr

and CeO_2 in an agate mortar. As starting materials, pure ZnO powders (99.9 % Fluka) and CeO_2 powders (99.9 % Fluka) were used. Pure ZnO powders and solid mixtures were first calcined at 600 and 650 ℃, respectively, for 24 h. After grinding and homogenization, pre-annealed mixtures were heat treated in air at 700, 800, 900 and 1000 ℃ for 48 h in alumina crucibles and without any compaction procedure. Finally, the samples were ground in an agate mortar to attain a uniform powder size. Then, samples were analyzed by X-ray diffraction (XRD) on a Bruker AXS D8 advanced diffractometer. Diffrac Plus and Win-Index programs were used to obtain information about the crystal structures of the samples. For comparison with standard data, Maint Powder Diffraction Database Manager Software program was used. In all cases, XRD patterns of the *monophase* samples were indexed on the basis of a hexagonal (wurtzite) structure in the CeO_2-ZnO binary system. Other samples, which were outside the solubility range, were heterogeneous solid mixtures having other phases that were indexed other than hexagonal. Morphologies of both non-annealed and annealed ZnO (at 1000 ℃) and doped *monophase* ZnO samples (annealed at 1000 ℃) were observed using a scanning electron microscope (SEM, LEO 440). After pressing them into pellets of 0.1 cm thickness (t) and 1.3 cm diameter (d) under $\sim$ 5 tons pressure the samples were calcined at 1000 ℃ for 12 h in air. After this heat treatment, XRD measurements showed no phase change in hexagonal samples. The average grain size was determined using Image-Pro plus 5.0 program by analyzing the SEM micrographs. For this purpose, ten grains were selected at random from each SEM micrograph. Electrical conductivity (σ) measurements of *monophase* samples (annealed at 1000 ℃) were made using the four-probe method. As in SEM measurements, the samples were also pressed into circular disks. To reduce contact resistance, fine platinum wires were directly attached to the sample surface. Measurements were carried out in the air at temperatures between 100 and 1000 ℃ (with 20 ℃ steps) for *monophase* samples. All experimental data were obtained by a Keithley 2400 SourceMeter and a Keithley 2700 Electrometer that were controlled by a computer [5].

3. Results and discussion

3.1. Structural analysis

Figure 1 shows the XRD patterns of undoped ZnO (after heating at 1000 ℃) and 1, 2, 3, 4, and 5 mol% CeO_2-doped ZnO samples (after heating at 1000 ℃). Figure 1 displays similar patterns for undoped and 1, 2 and 3 mol% CeO_2-doped ZnO, which can be indexed to the hexagonal (wurtzite) ZnO structure.

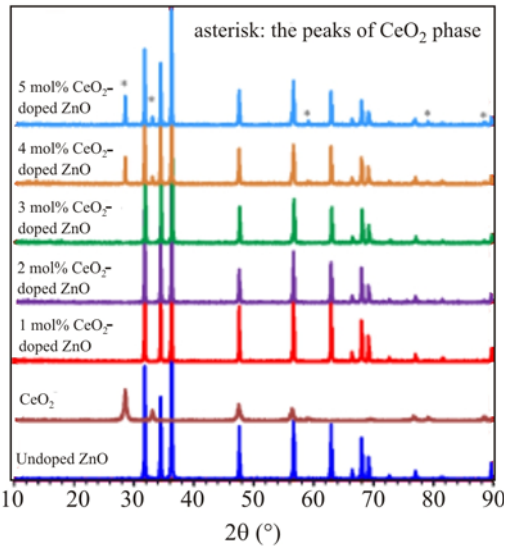

Fig. 1. XRD patterns of undoped ZnO, CeO_2 and CeO_2-doped ZnO samples (after heating at 1000 ℃).

In other words, the hexagonal ZnO structure is preserved up to 3 mol% CeO_2 doping. These types of samples with pure hexagonal structure are assigned as *H-phase*. However, cubic CeO_2 peaks can be clearly identified in Fig. 1 for 4 and 5 mol% CeO_2-doped ZnO.

For the hexagonal ZnO, lattice constants were determined at room temperature experimentally. The lattice constants of the *monophase* samples ranged from 3.2501 to 3.2603 Å for the a parameter and from 5.2069 to 5.2204 Å for the c parameter. Figure 2 shows the dependence of the lattice parameters a and c, respectively, on the mol fraction of CeO_2 additive. As can be seen, a and c increase with CeO_2 concentration. The ionic radius (four-coordinated) of the Ce^{4+} ion is 0.92 Å, while that of the Zn^{2+} is 0.74 Å [6]. Therefore, the increase in ZnO lattice parameters can be explained by this ionic radii difference.

Figure 3 shows typical SEM micrographs of non-annealed and annealed undoped ZnO (at 1000 ℃) and doped *monophase* ZnO samples. It can be seen that grains display homogeneous distribution for undoped ZnO samples. Average grain sizes were calculated to be 0.63 and 1.03 μm for non-annealed and annealed undoped ZnO samples, respectively. The grain sizes of the annealed samples are larger than of the non-annealed samples, which is caused by grain boundary surface energy reduction and can also be caused by strain relaxation. The heating treatment clearly produces a recovery of the crystal structure and an increase in the grain size. Also, it can be seen that the grains of the *monophase* samples have homogeneous distribution, and their values are about 1 μm.

3.2. Electrical conductivity

Total electrical conductivity is calculated using the

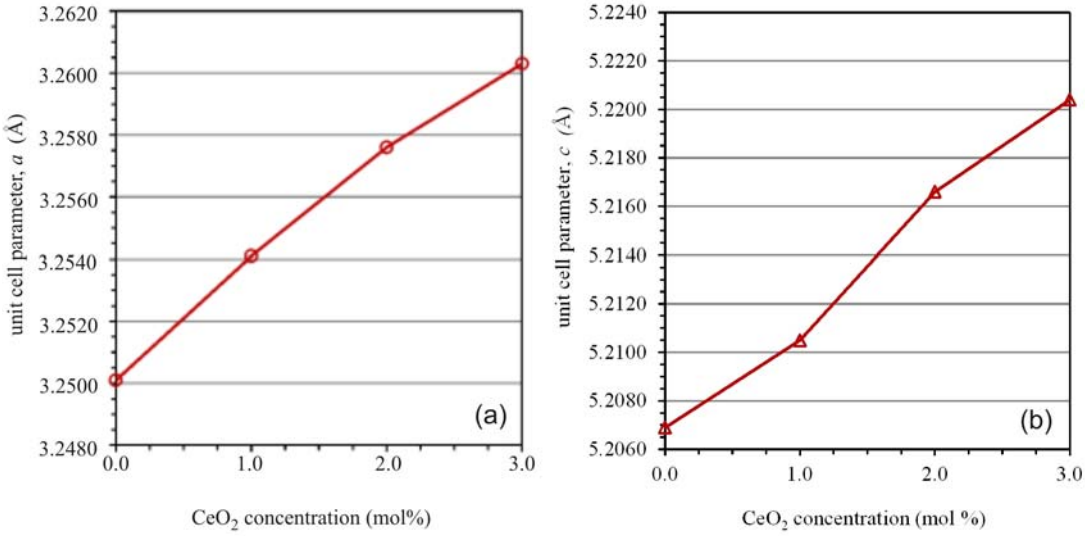

Fig. 2. Change in the unit cell parameters of *monophase* ZnO samples (after heating at 1000 °C).

Table 1. Observed phases in the binary system of CeO_2-doped ZnO (in the range of 1–10 mol%)

Temperature (°C)	CeO_2 addition (mol%)									
	1	2	3	4	5	6	7	8	9	10
1000	*H*	*H*	*H*	H + C	H + C	H + C	H + C	H + C	H + C	H + C

H: CeO_2-doped ZnO (*monophase*, hexagonal structure)
C: cubic CeO_2
H + C: heterogeneous solid mixtures (multiphase)

following equation:

$$\sigma = \frac{I}{V} G^{-1}, \tag{1}$$

where G is the geometric resistivity correction factor [7].

Electrical conductivity is related to the sample structure; any thermal treatment can modify the structural, and hence electrical properties. On this basis, the study of the temperature dependence of electrical properties may offer useful information about the possible changes to the structure and characteristics of the CeO_2-doped ZnO system [7, 8]. Pelleted *monophase* samples after heating at 1000 °C were studied in the temperature range of 100–1000 °C. $\text{Log}\,\sigma$ vs. $10^3/T$ graphs were drawn (Fig. 4) to assess the dependence of conductivity on temperature. As can be seen, the conductivity increases with measurement temperature, indicating semiconducting behaviour for all samples. ZnO is an *n*-type and non-stoichiometric semiconductor material owing to the presence of oxygen vacancies and interstitial zinc atoms (both are native defects) [9]. The electrical conductivity of pure ZnO is controlled via the intrinsic defects generated at high temperatures [10]. Also, in this figure, it is shown that the electrical conductivity increased with CeO_2 doping because the electron concentration of the system was increased with CeO_2 additive. Originating from extra electrons generated to compensate for the electric charge balance by adding Ce^{4+} for Zn^{2+}, the increased electron concentration gives rise to an increase in the electrical conductivity.

Also, in Fig. 4, the curves of the electrical conductivity of all the *monophase* samples have two linear and one transition region due to two competing processes. Thermal excitation process and oxygen adsorption occur simultaneously. At first, the electrical conductivity of all the *monophase* samples increases with temperature because the thermal excitation of electrons dominates over the oxygen adsorption process (this temperature range is 100–400 °C and 100–450 °C for undoped ZnO and all the *monophase* samples, respectively). The decrease in conductivity of the undoped ZnO (in the temperature range 400–550 °C) and of all the *monophase* samples (in the temperature range 450–550 °C) is attributed to vigorous adsorption of atmospheric oxygen on the sample surface. Beyond 550 °C, the conductivity increases probably due to the dominant thermal excitation of electrons

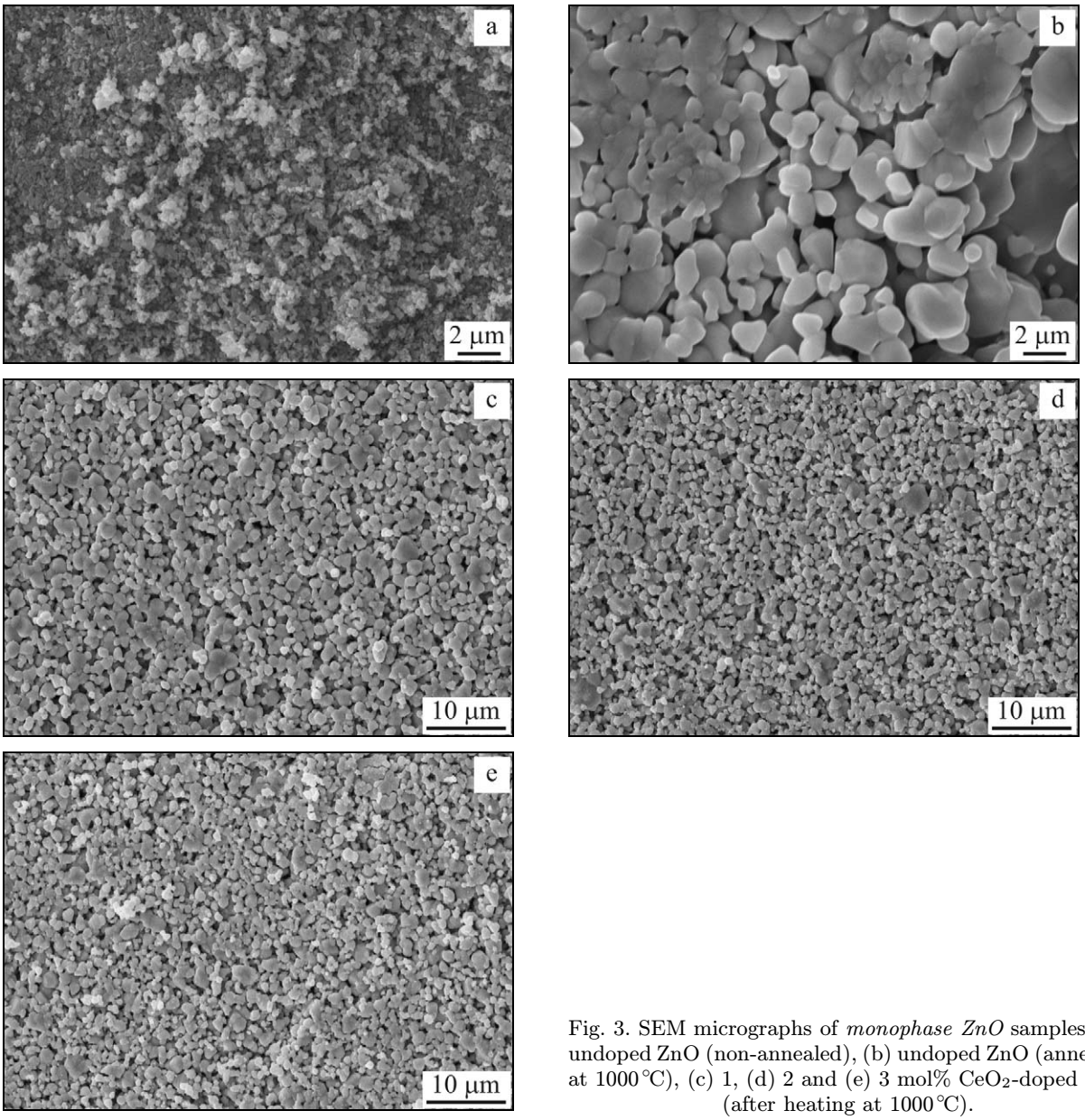

Fig. 3. SEM micrographs of *monophase ZnO* samples: (a) undoped ZnO (non-annealed), (b) undoped ZnO (annealed at 1000 °C), (c) 1, (d) 2 and (e) 3 mol% CeO_2-doped ZnO (after heating at 1000 °C).

and desorption of oxygen species [11]. The curves in Fig. 4 show that there may be more than one type of conduction mechanisms with the temperature variation for the undoped and all *monophase* samples. In the low-temperature region (100–400 °C and 100–450 °C for the undoped ZnO and all *monophase* samples, respectively) the electrical conductivity increases slowly with increasing temperature. The slow increase in the electrical conductivity may be associated with the hopping of carriers within localized states. In the high-temperature region (550–1000 °C), the electrical conductivity increases relatively faster with increasing temperature [12].

In general, for a semiconducting material, the conductivity increases exponentially with temperature indicating conductivity is a thermally activated process. For doped semiconductors with a low concentration of donors, hopping transport of carriers is expected between the nearest donors at low temperatures. Total electrical conductivity can be expressed as

$$\sigma = \sigma_0 \exp(-E_a/kT), \tag{2}$$

where σ is electrical conductivity, E_a is the activation energy that corresponds to the energy difference between the donor level and the conduction level, σ_0 is the so-called pre-exponential factor, k is the Boltzmann constant, and T is the absolute temperature [4]. The activation energy can then be calculated using the relation:

$$\log \sigma = -\frac{E_a}{k}\frac{1}{T} + \log \sigma_0. \tag{3}$$

Table 2. Activation energy values of *monophase* ZnO samples (after heating at 1000 °C)

CeO_2 addition (mol%)	Activation energy, E_a (eV)	
	E_{a1} (100–450 °C)*	E_{a2} (550–1000 °C)
Undoped ZnO	0.458	0.989
1	0.392	1.131
2	0.331	1.128
3	0.302	1.132

*this temperature range is 100–400 °C for undoped ZnO

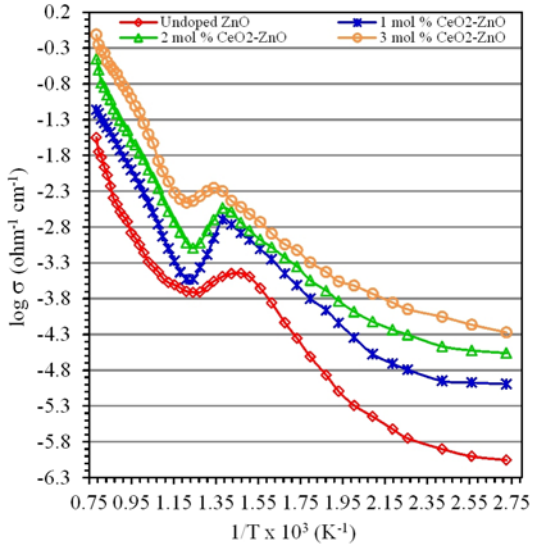

Fig. 4. Electrical conductivity plots for undoped ZnO (annealed at 1000 °C) and *monophase* ZnO samples (after heating at 1000 °C).

The slope of the linear part of the Arrhenius curve of the $\log\sigma$ vs. $10^3/T$ graph is equal to $-E_a/k$. The activation energy values can be calculated for all the *monophase* ZnO samples (Table 2) from the curves. It is shown that the activation energy in both low and high-temperature region decreases with decreasing mol fraction of CeO_2. From Table 2, it can be seen that the activation energy in the low-temperature region is less than the energy in the high-temperature region because material passes from one conduction mechanism to another. At high temperatures, the electrical conductivity is mainly determined by the intrinsic defects and is called as intrinsic conduction. The high values of activation energy in this region may be attributed to the fact that the energy needed to form the defects is much larger than the energy required for its drift. That is why the intrinsic defects caused by the thermal fluctuations determine the electrical conductivity of the samples at high temperatures [13].

4. Conclusion

CeO_2-doped ZnO powders have been synthesized by the solid state method. The solubility limit of CeO_2 in ZnO lattice (after heating at 1000 °C) is 3 mol%. Because Ce^{4+} ions substitute for Zn^{2+} ions in ZnO crystal structure and generate extra electrons, the electrical conductivity of *monophase* samples increased with CeO_2 doping.

Acknowledgements

This study was financially supported by Cankiri Karatekin University Dean of Science Faculty. The author is thankful to Mehmet Bozoklu, who is a Ph.D. student at Erciyes University, Institute of Natural and Applied Sciences, Department of Physics.

References

[1] Mereu, R. A., Mesaros, A., Vasilescu, M., Popa, M., Gabor, M. S., Ciontea, L., Petrisor, T.: Ceram. Int., *39*, 2013, p. 5535. doi:10.1016/j.ceramint.2012.12.067
[2] Fang, F., Ng, A. M. C., Chen, X. Y., Djurisic, A. B., Zhong, Y. C., Wong, K. S., Fong, P. W. K., Lui, H. F., Surya, C., Chan, W. K.: Mater. Chem. Phys., *125*, 2011, p. 813. doi:10.1016/j.matchemphys.2010.09.051
[3] Wang, L., Pu, Y., Fang, W., Dai, J., Zheng, C., Mo, C., Xiong, C.: Thin Solid Films, *491*, 2005, p. 323. doi:10.1016/j.tsf.2005.05.048
[4] Colak, H., Turkoglu, O.: Mater. High Temp., *29*, 2012, p. 344. doi:10.3184/096034012X13390873728509
[5] Colak, H., Turkoglu, O.: J. Mater. Sci. Technol., *27*, 2011, p. 944. doi:10.1016/S1005-0302(11)60168-0
[6] Weast, R. C.: Handbook of Chemistry and Physics. Cleveland, CRC Press 1975–1976.
[7] Yilmaz, S., Turkoglu, O., Belenli, I.: Mater. Chem. Phys., *112*, 2008, p. 472. doi:10.1016/j.matchemphys.2008.06.002
[8] Lee, J. B., Lee, H. J., Seo, S. H., Park, J. S.: Thin Solid Films, *398–399*, 2001, p. 641. doi:10.1016/S0040-6090(01)01332-3
[9] Liu, Y., Lao, L. E.: Solid State Ionics, *177*, 2006, p. 159. doi:10.1016/j.ssi.2005.10.002
[10] Colak, H., Turkoglu, O.: J. Mater Sci: Mater. Electron., *23*, 2012, p. 1750. doi:10.1007/s10854-012-0657-1

[11] Prajapati, C. S., Sahay, P. P.: Appl. Surf. Sci., *258*, 2012, p. 2823. doi:10.1016/j.apsusc.2011.10.141
[12] Rahman, M. M., Khan, M. K. R., Islam, M. R., Halim, M. A., Shahjahan, M., Hakim, M. A., Saha, D. K., Khan, J. U.: J. Mater. Sci. Technol., *28*, 2012, p. 329. doi:10.1016/S1005-0302(12)60064-4
[13] Patil, A. V., Dighavkar, C. G., Sonawane, S. K., Patil, S. J., Borse, R. Y. J.: Optoelectron. Biomed. Mater., *1*, 2009, p. 226.